Proceedings of the 17th World Congress
The International Federation of Automatic Control
Seoul, Korea, July 6-11, 2008

Design Parameter Analysis of a Roll-to-Roll Printing Machine

Chul-Goo Kang* and Bong-Ju Lee**

**Dept of Mechanical Engineering, Konkuk University, Gwangjin-gu, Seoul 143-701, Korea (Tel:+82-2-447-2142; e-mail: cgkang@konkuk.ac.kr).*
***Dept of Mechanical Engineering, Konkuk University, Gwangjin-gu, Seoul 143-701, Korea (e-mail: kk103@konkuk.ac.kr).*

Abstract: The stability of multi-input and multi-output web-tension systems is an important factor that is required for the roll-to-roll printing machines. This paper analyzes stability for design parameters of a web-tension system of a high-speed gravure printing machine. Analyzed parameters include moment of inertia of the passive dancer, viscous friction coefficient of the dancer system, distances from hinge to dancer roller and cylinder, and proportional gains of the tension control system. The validity of the analysis is demonstrated by simulation study.

1. INTRODUCTION

Large printing demand of our modern society requests development of high-speed printing machines. A reasonable model for web tension plays an important role for the development of a high-speed roll-to-roll printing machine.

Web tension control is a prerequisite for accurate register control to obtain high printing resolution (Gravure Education Foundation, 2003). If web tension in roll-to-roll printing machine is too high, several problems occur such as large register error, rewinder wrinkling, web tearing, and plastic deformation of the web. On the other hand, if web tension is too small, then problems occur such as web oscillations, loose rewinding and web surface damages.

Usually highly interactive web tension is modeled under the assumption that the span length is fixed (Shin, 2000; Shin, 1995; Mathur et al., 1998; Weiss, 1985), but at unwinder and rewinder units using turrets, the span length is changing from time to time.

In this paper, we analyze design parameters of the tension control system of the gravure printing machine. Furthermore, we analyze the stability of web-tension model for specific parameters (such as web speed or moment of inertia of dancer arm) using eigenvalues of the linearized model. The validity of the stability analysis is demonstrated by means of simulation study.

2. GRAVURE PRINTING MACHINE

Fig. 1 shows schematic diagram of the pilot plant of the gravure printing machine with three color printing function installed at Flexible Display Roll-to-Roll Research Center (FDRC), Konkuk University (manufactured by SAM, Inc.). This system is composed of an unwinder unit including turret and splicing mechanism and a passive dancer, an infeeder unit with a passive dancer, three printing units with color register control devices, an outfeeder unit with a passive dancer, and a rewinder unit including an active dancer. Dancers may be bypassed optionally. Eight loadcells are installed at idle rollers in the middle of continuous process for tension pickup.

When a command is given at HMI in the figure, PLC generates appropriate command signals for motion control of each motor, and then the controller of each motor controls tensions and speeds of the web using motion commands and feedback signals for motion and web tension.

In this pilot plant, web speed, angular velocity of driving rolls, web tension, angular speed of the turret, radius of the wound roll, arm angles of the dancers can be measured and monitored through control panels and also PCs.

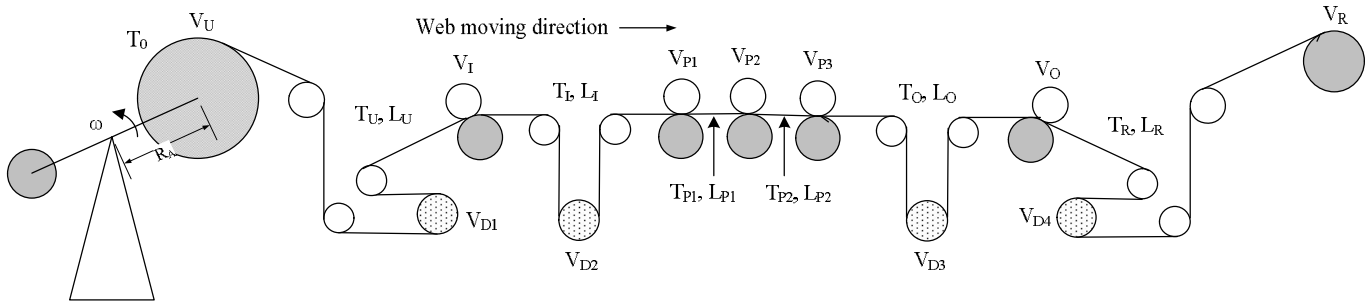

Fig. 1 Schematic diagram of the gravure printing machine.

3. NONLINEAR TENSION MODEL

In this paper, we derive a nonlinear MIMO model which represents actual dynamics of transient region and turret operation. In the equations, V_i represents web speed, T_i does web tension, V_{D1}, V_{D2}, V_{D3}, V_{D4} represent speeds of dancers. Subscripts U, I, O, R imply unwinder, infeeder, outfeeder, rewinder, respectively.

Within one span, cross sectional area and velocity of the web may vary continuously, but tension and strain are assumed to be constants along web longitudinal direction. All these variables may vary in time.

Under these conditions, we obtain the following equations from mass conservation law.

$$\frac{d}{dt}\left(\int_{x_1}^{x_2}\rho(x,t)A(x,t)dx\right)=\rho_1(t)A_1(t)V_1(t) - \rho_2(t)A_2(t)V_2(t) \tag{1}$$

where x implies web position in longitudinal direction, ρ implies the density of the web, A implies cross sectional area of the web, subscripts $_{1,2}$ imply the positions of the upstream roller and downstream roller.

Representing Eq. (1) by means of web strain ε, we obtain the following equation.

$$\frac{d}{dt}\left[\frac{L(t)}{1+\varepsilon_2(t)}\right]=\frac{V_1(t)}{1+\varepsilon_1(t)}-\frac{V_2(t)}{1+\varepsilon_2(t)} \tag{2}$$

The strain of the web is very small in general. Thus, assuming ε is much smaller than 1 in Eq. (2), we can approximately rewrite it as follows.

$$\frac{d}{dt}\left[\left(1-\varepsilon_2(t)\right)L(t)\right]=\left[1-\varepsilon_1(t)\right]V_1(t) - \left[1-\varepsilon_2(t)\right]V_2(t) \tag{3}$$

From Hooke's law for the web, the following equation can be obtained.

$$T(t)=A(x,t)\,E(x,t)\,\varepsilon(t) \tag{4}$$

where E implies Young's modulus that may vary a little due to the effects of temperature, humidity, etc.

Substituting Eq. (4) for Eq. (3), and using average value AE instead of $A(x,t)E(x,t)$, we obtain a new nonlinear tension model that is able to consider web length variation within a span.

$$L(t)\frac{dT_2(t)}{dt}=V_1(t)T_1(t)-\left[V_2(t)+\frac{dL(t)}{dt}\right]T_2(t) + AE\left[V_2(t)-V_1(t)+\frac{dL(t)}{dt}\right] \tag{5}$$

In general, variation of $A(x,t)E(x,t)$ is very small in a roll-to-roll printing machine. Thus, using the average value AE instead of $A(x,t)E(x,t)$ is acceptable for representing dynamic characteristics of the system.

In the following equation, θ_D represents the angle of the dancer arm from a neutral position, d_D represents the length of the dancer arm from hinge to dancer roller, d_P represents the length of the dancer from hinge to pneumatic piston, and P_0 and A_P represent pneumatic pressure and piston area, respectively. The pneumatic cylinder used for dancer system in general is preloaded by a spring within the cylinder.

From the free body diagram for the dancer roller, the following equation of motion is obtained (Lee et al., 2005).

$$J_D\dot{V}_D=(T_{U2}-T_{U1})r_D^2-b_DV_D \tag{6}$$

where r_D implies the radius of dancer roller, b_D does the coefficient of viscous friction of dancer roller, and V_D does web speed at dancer roller. We assume no slip between dancer rollers and web materials.

Then, applying Newton's law of motion to the free body diagram of the dancer arm, we can obtain the following equation.

$$J_{eq}\ddot{\theta}_D=-(m_Dd_D\ddot{\theta}_D+T_{U1}+T_{U2})d_D+P_0A_P - \left[\frac{F_{\max}-F_{\min}}{x_{p\max}}\left(\frac{x_{p\max}}{2}+d_P\theta_D\right)+F_{\min}\right]d_P - b_{eq}\dot{\theta}_D \tag{7}$$

where J_{eq} represents the equivalent moment of inertia of the dancer arm with respect to hinge center, b_{eq} does the equivalent coefficient of viscous friction of the dancer arm, and m_D does the mass of dancer roller. And $F_{\max}, F_{\min}$ represent maximum and minimum compression force of the spring, and $x_{p\max}$ does maximum stroke of the piston.

If we neglect mass, moment of inertia, and viscous friction of dancer roller in Eqs. (6) and (7), then $T_{U1}=T_{U2}=T$, and we can obtain the following equation for the roller.

$$J_{eq}\ddot{\theta}_D+b_{eq}\dot{\theta}_D+\frac{F_{\max}-F_{\min}}{x_{p\max}}d_P^2\theta_D = (P_0A_P-\frac{F_{\max}+F_{\min}}{2})d_P-2Td_D \tag{8}$$

Applying web-tension model, Eq. (5), and dancer model,

Eq. (8) for the 3 color printing machine results in the following nonlinear MIMO plant model, in which $\dot{l}_U, \dot{l}_R$ are constant linear speeds by unwind and rewind turrets.

$$
\begin{aligned}
&L_U\dot{T}_U = V_U T_{U0} - (V_I + \dot{L}_U)T_U + (V_I - V_U + \dot{L}_U)AE \\
&\dot{L}_U = \dot{l}_U + 2d_D\dot{\theta}_{D1}, \quad \dot{l}_U = \mathcal{V}_U \text{ (given)} \\
&L_I\dot{T}_I = V_I T_U - (V_{P1} + \dot{L}_I)T_I + (V_{P1} - V_I + \dot{L}_I)AE \\
&\dot{L}_I = 2d_D\dot{\theta}_{D2} \\
&J_{eq}\ddot{\theta}_{D2} + b_{eq}\dot{\theta}_{D2} + \frac{F_{\max} - F_{\min}}{x_{p\max}} d_P^2\theta_{D2} = \\
&\quad (P_{I0}A_P - \frac{F_{\max} + F_{\min}}{2})d_P - 2T_I d_D \\
&L_{P1}\dot{T}_{P1} = V_{P1}T_I - V_{P2}T_{P1} + (V_{P2} - V_{P1})AE \\
&L_{P2}\dot{T}_{P2} = V_{P2}T_{P1} - V_{P3}T_{P2} + (V_{P3} - V_{P2})AE \\
&L_O\dot{T}_O = V_{P3}T_{P2} - (V_O + \dot{L}_O)T_O + (V_O - V_{P3} + \dot{L}_O)AE \\
&\dot{L}_O = 2d_D\dot{\theta}_{D3} \\
&J_{eq}\ddot{\theta}_{D3} + b_{eq}\dot{\theta}_{D3} + \frac{F_{\max} - F_{\min}}{x_{p\max}} d_P^2\theta_{D3} = \\
&\quad (P_{O0}A_P - \frac{F_{\max} + F_{\min}}{2})d_P - 2T_O d_D \\
&L_R\dot{T}_R = V_O T_O - (V_R + \dot{L}_R)T_R + (V_R - V_O + \dot{L}_R)AE \\
&\dot{L}_R = \dot{l}_R + 2d_D\dot{\theta}_{D4}, \quad \dot{l}_R = \mathcal{V}_R \text{ (given)} \\
&J_{eq}\ddot{\theta}_{D4} + b_{eq}\dot{\theta}_{D4} + \frac{F_{\max} - F_{\min}}{x_{p\max}} d_P^2\theta_{D4} = \\
&\quad (P_{R0}A_P - \frac{F_{\max} + F_{\min}}{2})d_P - 2T_R d_D
\end{aligned}
\tag{9}
$$

4. LINEARIZATION

It is not easy to check stability of the nonlinear plant models, Eqs. (9). For the purpose of stability analysis, therefore, we linearize the nonlinear model. First, defining state variables as $x_1 = T_U$, $x_2 = \theta_{D1}$, $x_3 = \dot{\theta}_{D1}$, $x_4 = T_I$, $x_5 = \theta_{D2}$, $x_6 = \dot{\theta}_{D2}$, $x_7 = T_{P1}$, $x_8 = T_{P2}$, $x_9 = T_O$, $x_{10} = \theta_{D3}$, $x_{11} = \dot{\theta}_{D3}$, $x_{12} = T_R$, $x_{13} = \theta_{D4}$, $x_{14} = \dot{\theta}_{D4}$, Eq. (9) results in the following nonlinear state equation that has 14 state variables and 7 input variables.

$$\dot{\mathbf{x}}(t) = \mathbf{f}(\mathbf{x}(t), \mathbf{u}(t), t) \tag{10}$$

where input vector is $\mathbf{u} = [V_U, V_I, V_{P1}, V_{P2}, V_{P3}, V_O, V_R]^T$. Let operating point as $x_1^* = T_U^*$, $x_2^* = \theta_{D1}^* = 0$, $x_3^* = \dot{\theta}_{D1}^* = 0$, $x_4^* = T_I^*$, $x_5^* = \theta_{D2}^* = 0$, $x_6^* = \dot{\theta}_{D2}^* = 0$, $x_7^* = T_{P1}^*$, $x_8^* = T_{P2}^*$, $x_9^* = T_O^*$, $x_{10}^* = \theta_{D3}^* = 0$, $x_{11}^* = \dot{\theta}_{D3}^* = 0$, $x_{12}^* = T_R^*$, $x_{13}^* = \theta_{D4}^* = 0$, $x_{14}^* = \dot{\theta}_{D4}^* = 0$, and $\mathbf{u}^* = [V_U^*, V_I^*, V_{P1}^*, V_{P2}^*, V_{P3}^*, V_O^*, V_R^*]^T$. Then the following linearized state equation is obtained.

$$\dot{\mathbf{x}}(t) = \mathbf{A}\mathbf{x}(t) + \mathbf{B}\mathbf{u}(t) \tag{11}$$

where **A** is 14×14 state matrix, and **B** is 14×7 input matrix.

5. DESIGN PARAMETER ANALYSIS

To analyze plant stability of the roll-to-roll printing machine for increasing web speed, we calculate eigenvalues of the matrix **A** in Eq. (11). Parameter values used here for the actual gravure printing machine are: A=20×10^{-6}, E=2.1×10^{9}, L_{U1}=3.78, L_{U2}=2.34, L_{I1}=1.34, L_{I2}=4.33, L_{P1}=9.55, L_{P2}=10.22, L_{O1}=8.22, L_{O2}=3.73, L_{R1}=1.26, L_{R2}=4.80, d_D=0.3, d_P=0.15, m_D=9.676, J_D=0.0295, r_D=0.06, b_D=0.0005, A_P=0.00273. All units used here are SI units.

When web speed is 100 mpm (meter/min), 14 eigenvalues are calculated. We let $T_U^* = 100N/m$, $T_I^* = 110N/m$, $T_O^* = 120N/m$, $T_R^* = 50N/m$. Since all eignevalues have negative real parts, the plant model is stable. But it is near marginal stability since there is quadruple -0.008 eigenvalues.

In order to estimate stability behavior for increasing web speed, we calculate eigenvalues for web speed 100 mpm, 200 mpm, 300 mpm, 400 mpm, and 500 mpm. From this result, we find that the eigenvalues of web plant model moves to the left in s-plane as web speed increases, and therefore the stability of web plant model improves as web speed increases.

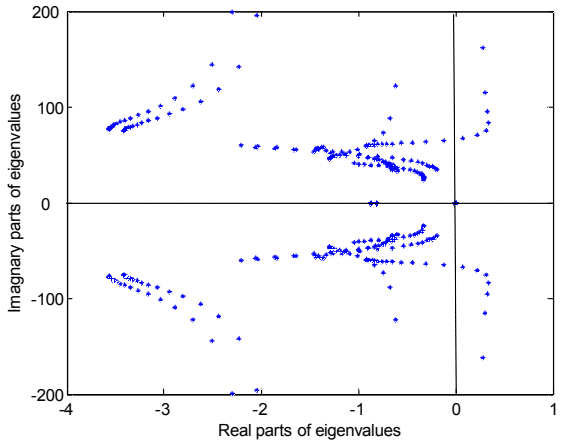

Fig. 2 Eigenvalue trajectories for inertia variations of the dancer arm (500 mpm).

Fig. 2 shows eigenvalue trajectories for inertia variations of the dancer arm, in which eigenvalues for each J_{eq} are calculated at every 0.1 increments from J_{eq} = 0.0004 to 2.0004. This result shows that eigenvalues move to the left in s-plane as J_{eq} value increases, and thus the plant system becomes stable as J_{eq} is bigger than a certain value (about 0.7 for the present case). Furthermore, it becomes more stable as J_{eq} becomes bigger.

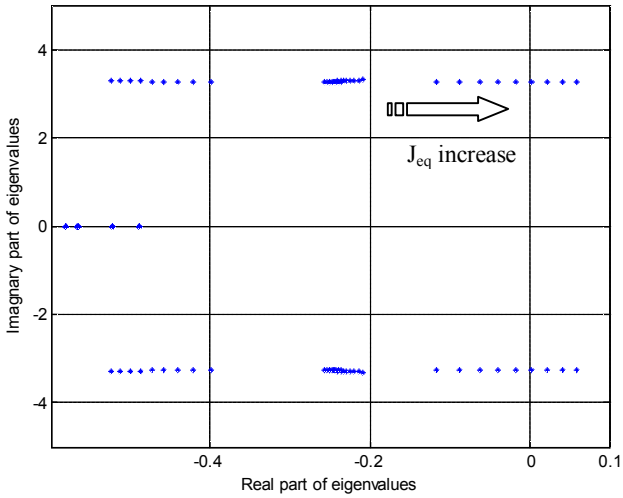

Fig. 3 Eigenvalue trajectories for inertia variations of the dancer arm (300 mpm).

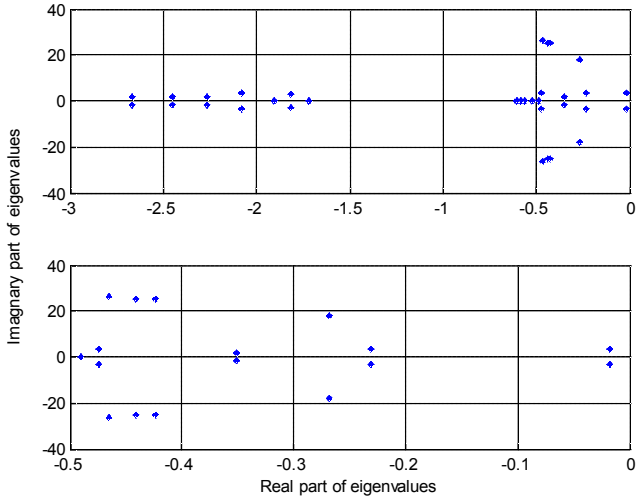

Fig. 4 Eigenvalue trajectories for viscous friction coefficient changes of the dancer mechanism

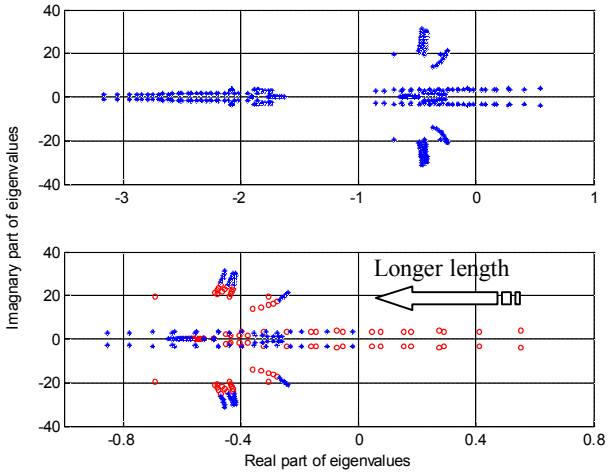

Fig. 5 Eigenvalue trajectories for variations of piston to hinge distance d_P

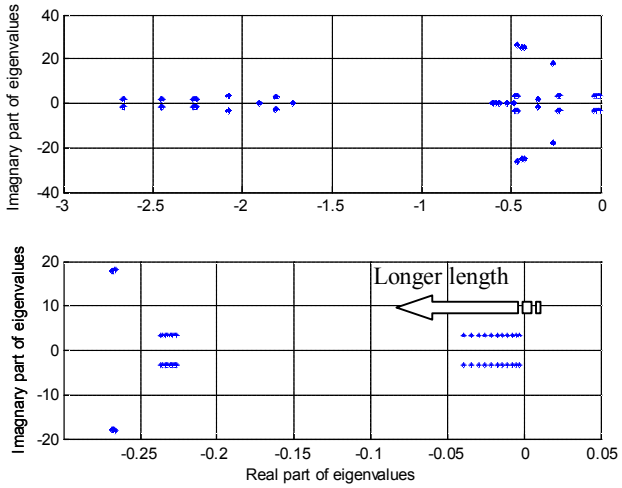

Fig. 6 Eigenvalue trajectories for variations of dancer roller to hinge distance d_D

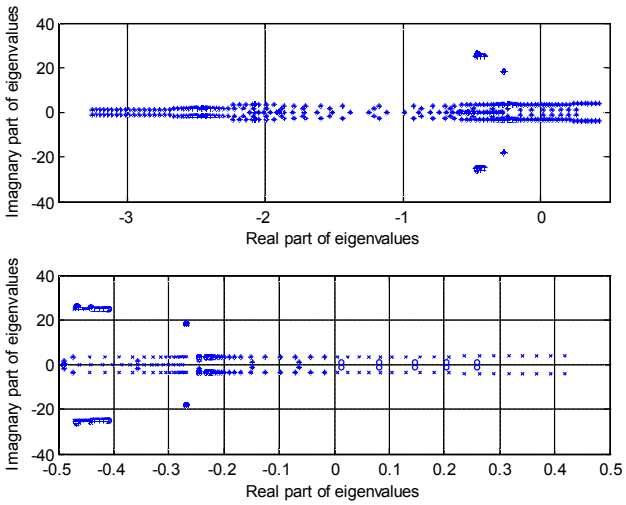

Fig. 7 Eigenvalue trajectories for unwinder P gain (K_{UP}) changes

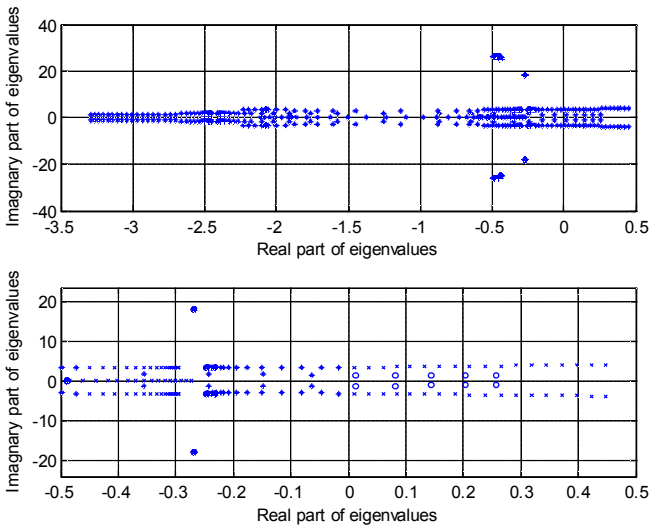

Fig. 8 Eigenvalue trajecgtories for infeeder P gain (K_{IP}) changes

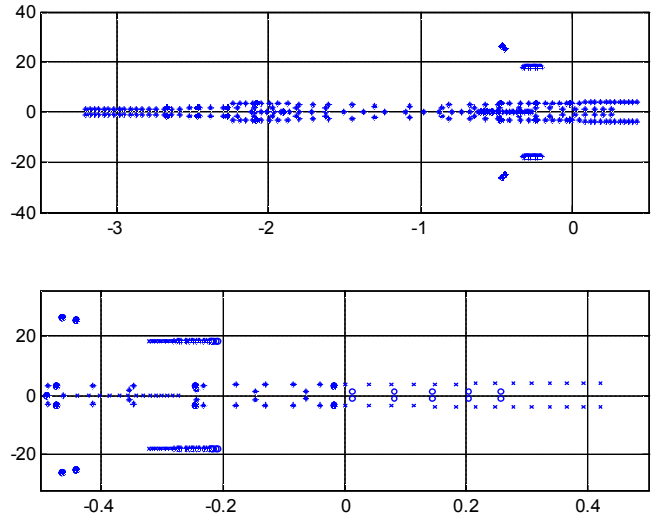

Fig. 9 Eigenvalue trajectories for outfeeder P gain (K_{OP}) changes

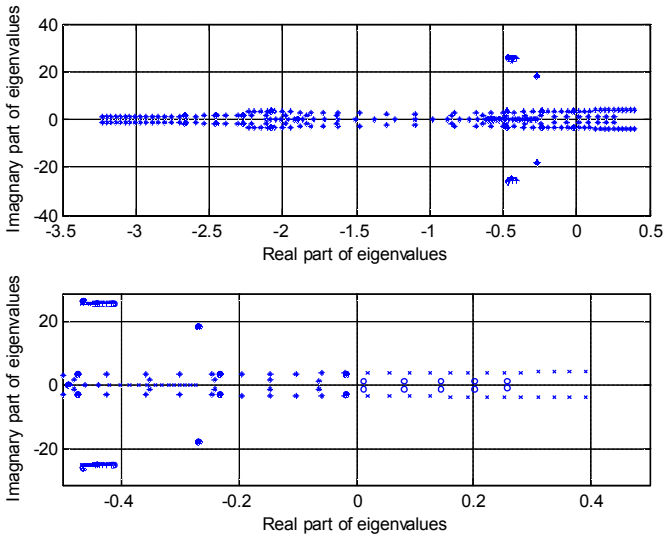

Fig. 10 Eigenvalue trajectories for rewinder P gain (K_{RP}) changes

Fig. 3 shows eigenvalue trajectories for inertia changes of the dancer arm from 1.9 to 5.9 kg·m^2, when web speed is 300 mpm. From this result, we see that the system is stable if J_{eq} is less than 4.5 kg·m^2 when web speed is 300 mpm.

Fig. 4 shows eigenvalue trajectories for viscous friction coefficient changes from 0.0001 to 0.001 N·s/m, and the plant stability is less sensitive for viscous friction coefficient variation. The plant is stable for viscous friction coefficient changes from 0.0001 to 0.001 N·s/m when web speed is 300 mpm.

Fig. 5 shows eigenvalue trajectories for variations of piston to hinge distance d_P from 0.1 to 0.2 m with d_D = 0.3 m and web speed = 300 mpm. Fig. 6 shows eigenvalue trajectories for variations of dancer roller to hinge distance d_D from 0.2 to 0.3 m with d_P = 0.15 m and web speed = 300 mpm. From these results, the pant stability is improved as the lengths, d_P and d_D are longer.

Fig. 7 shows eigenvalue trajectories for unwinder P gain (K_{UP}) changes from 0.06 to 0.21 with all other P gains = 0.2 for the PI control system and web speed = 500 mpm. Fig. 8 shows eigenvalue trajectories for infeeder P gain (K_{IP}) changes from 0.06 to 0.21 with all other P gains = 0.2, Fig. 9 shows eigenvalue trajectories for outfeeder P gain (K_{OP}) changes from 0.06 to 0.25 with all other P gains = 0.2, and Fig. 10 shows eigenvalue trajectories for rewinder P gain (K_{RP}) changes from 0.06 to 0.26 with all other P gains = 0.2. From these figures, we see that the proportional gains of the PI web tension control system should be less than some limiting values to obtain appropriate stability of the feedback control system.

The following Fig. 11 shows a simulation result using Eq. (9) via Simulink when there exit 1 % initial condition errors at web tension. Upper figure of Fig. 11 shows simulated tension of unwind zone for web speed of 100 and 500 mpm with sinusoidal disturbance from unwind roll when there exist no initial condition errors. Lower figure of Fig. 11 shows simulated tension of unwind zone for 100 and 500 mpm speed with the same condition as above when there exist 1% initial condition errors of steady-state tension values. The result in Fig. 11 demonstrates that the derived web-tension model is stable, and also the plant stability improves as web speed increases.

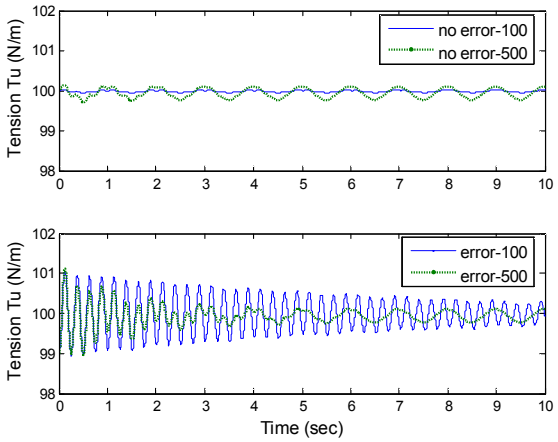

Fig. 11 Time responses for initial condition errors exists

5. CONCLUSION

In this paper, we have shown a nonlinear web-tension model that can consider span length variation due to dancer, and have analyzed design parameters using eigenvalue trajectories of the linearized model about operating conditions. The linearized system with 14×14 system matrix neglects mass, moment of inertia and viscous friction of dancer roller itself. Furthermore, the plant model becomes more stable as web speed increases, differently as expected.

Eigenvalues for parameter J_{eq} move to the left in s-plane from the right half plane as J_{eq} value increases, and thus the plant system becomes stable as J_{eq} is bigger than a certain value (about 0.7 for the present case). Moreover, it becomes more stable as J_{eq} becomes bigger. Furthermore, it is shown that plant stability is less sensitive for viscous friction

coefficient variation compared to dancer arm inertia, and is improved as the lengths from hinge to cylinder and dancer roller, d_P and d_D are longer. Also it is shown that the proportional gains of the PI web tension control system should be less than some limiting values to obtain appropriate stability of the feedback control system.

ACKNOWLEDGEMENT

The author gratefully acknowledges the financial support from Seoul R&BD Program (e-Printing Cluster; Project Number: 10848).

REFERENCES

Dwivedula, R. V., et al., Control Engineering Practice, Elsevier, pp. 489~498, 2003.

Gravure Education Foundation and Gravure Association of America, *Gravure Process and Technology*, pp. 291~335, 2003.

Lee, Bong-Ju and Chul-Goo Kang, "Roll change modeling and tension control performance improvement of a high-speed printing machine," *Proc. of the Annual Fall Meeting of KSME*, pp. 2663-2667, 2005.

Mathur, Priyadarshee D. and William C. Messner, "Controller Development for a Prototype High-Speed Low-Tension Tape Transport," *IEEE Transactions on control system technology,* Vol. 6. No. 4, pp 534~542, 1998.

Shin, K., "Non-Interacting Tension Control in a Multi-Span Web Transport System," *Trans. KSME*, Vol. 19 No. 10, pp. 2548~2554, 1995.

Shin, K., Tension Control, *TAPPI Press,* 2000.

Weiss, Herbert L., *Rotogravure and Flexographic Printing Presses*, Converting Technology Corp., pp. 307~446, 1985.